Plant Cysteine Oxidase oxygen-sensing function is conserved in early land plants and algae

Leah J. Taylor-Kearney[a,c], Samuel Madden[a], Jack Wilson[a,d], Elisabete Pires[a], Philip Holdship[b], Anthony Tumber[a], Rosalind E. M. Rickaby[b] and Emily Flashman[a*]

[a] Chemistry Research Laboratory, University of Oxford, 12 Mansfield Road, Oxford, OX1 3TA, United Kingdom

[b] Department of Earth Sciences, University of Oxford, South Parks Road, Oxford OX1 3AN, United Kingdom

[c] Present address: University of California, Berkeley, CA 94720, United States of America

[d] Present address: Nuclear Futures Institute, University of Bangor, Dean Street, Bangor, LL57 1UT, United Kingdom

[*] To whom correspondence should be addressed: emily.flashman@chem.ox.ac.uk

Abstract

All aerobic organisms require O_2 for survival. When their O_2 is limited (hypoxia), a response is required to reduce demand and/or improve supply. A hypoxic response mechanism has been identified in flowering plants: stability of proteins with N-terminal cysteine residues is regulated in an O_2-dependent manner by the Cys/Arg branch of the N-degron pathway. Oxidation of these cysteine residues is catalysed by plant cysteine oxidases (PCOs) which destabilises proteins in normoxia; PCO inactivity in hypoxia results in protein stabilisation. Biochemically, the PCOs are sensitive to O_2 availability and can therefore act as plant O_2 sensors and regulation of the stability of proteins such as Group VII ethylene response factors (ERF-VIIs) can initiate adaptive responses to hypoxia. It is not known whether oxygen-sensing mechanisms exist in other phyla from the plant kingdom. Known PCO targets are only conserved in flowering plants, however PCO-like sequences are conserved in all planta. We sought to determine whether PCO-like enzymes from the liverwort, *Marchantia polymorpha* (MpPCO) and the freshwater algae, *Klebsormidium nitens* (KnPCO) have a similar function to PCO enzymes from *Arabidopsis thaliana*. We report that MpPCO and KnPCO show O_2-sensitive N-terminal cysteine dioxygenase activity towards known AtPCO ERF-VII substrates as well as a putative endogenous substrate, MpERF-like, which was identified by homology to the Arabidopsis ERF-VIIs transcription factors. This work confirms functional and O_2-dependent PCOs from Bryophyta and Charophyta, indicating the potential for PCO-mediated O_2-sensing pathways in these organisms and suggesting PCO O_2-sensing function could be important throughout the plant kingdom.

Keywords: enzyme kinetics, evolution, hypoxia, N-degron pathway, oxidase, post-translational modification.

Introduction

O_2 is a molecule that has shaped evolution [1,2]. Across modern surface environments, a range of niches of varying degrees of oxygenation persist. Such evolutionary, temporal and spatial variability in oxygenation likely requires both long- and short-term organismal adaptation to O_2 availability. The primary mechanism by which higher plants sense and adapt to low O_2 availability has been established over recent years [3–5]. O_2-sensing enzymes, the Plant Cysteine Oxidases (PCOs), catalyse oxidation of cysteine to Cys-sulfinic acid at the N-termini of target proteins, a reaction whose rate is dependent on the availability of molecular O_2 [6–8]. Co-translational methionine cleavage exposes the N-terminal Cys for oxidation, leading to the degradation of the target protein via the Cys/Arg branch of the N-degron pathway [9,10]: Oxidised N-terminal Cys residues are substrates for arginyl transferase enzymes, with the arising arginylated N-termini recognised by ubiquitin ligases. Ubiquitination signals for the protein to be degraded by the proteasome [11,12]. This pathway therefore connects O_2 availability and destabilisation of target proteins, while in low O_2 (hypoxic) conditions these proteins remain stable.

PCO target proteins, identified in Arabidopsis, include the ERF-VIIs which are involved in responses to submergence-induced acute hypoxia and are defined by their MCGGAI N-termini [9,10]. Also identified to date are proteins related to plant development, Vernalisation 2 (AtVRN2) involved in cold-induced suppression of flowering [13] and AtZPR2 which regulates activity in the hypoxic shoot meristem [14]. Each of these O_2-signalling mechanisms regulated by the PCOs is arguably unique to flowering and perhaps seeding plants, with evolutionary analysis of substrates limiting their presence to angiosperms and some spermatophytes [15]. Interestingly, PCO-like sequences are conserved in early land plants and algae [15], while a homologous enzyme, HsADO, has been reported as regulating the stability of N-terminal Cys-initiating proteins in humans [16]. This suggests that Nt-Cys dioxygenase function may be an evolutionary conserved mechanism of O_2 sensing [17].

To investigate this possibility, we have expressed PCO-like enzymes from *Marchantia polymorpha*, representing early land plants, and the filamentous freshwater algae *Klebsormidium nitens* (also known as *Klebsormidium flaccidum*). *M. polymorpha* is a liverwort, whose ancestor is reputed to be the first land plant and which possibly retains features of both its algal ancestors and extant land plants [18]. *K. nitens* is an undifferentiated semiterrestrial freshwater alga and is a model for understanding the early transition to land [19]. We show that the MpPCO and KnPCO enzymes are functionally homologous to the Arabidopsis PCOs and identify a putative endogenous substrate for MpPCO. We show that MpPCO and KnPCO enzyme activity is O_2-dependent, with KnPCO activity highly sensitive to changes in O_2 availability. Crucially, both enzymes demonstrate the potential, at least biochemically, for a conserved O_2-sensing function in early plants and raising the possibility that O_2 sensing is important in the life of aquatic and early land plants.

Results

Identification, purification and characterisation of MpPCO and KnPCO

MpPCO and KnPCO sequences were identified through BLASTp searches of available proteome and genome portals using AtPCO 1- 5 as input sequences. Both species contained only one PCO-like sequence, rather than multiple sequences observed in higher plants [15]. Sequence alignment of MpPCO and KnPCO revealed that they are highly conserved with those of the AtPCOs. MpPCO shares the greatest homology with AtPCO4 at 49.6 % identity, while KnPCO shares 43.5% identity with AtPCO1. KnPCO and MpPCO retain key residues relevant to structure and function, for example three

iron-binding His residues and conserved Asp and Tyr residues close to the active site known to be important for PCO catalytic activity [20] (Supplementary Figure S1).

Expression and purification of MpPCO and KnPCO followed protocols previously described for the AtPCOs [8]. Recombinant proteins were purified via Ni-affinity chromatography and size exclusion chromatography to >95% purity as judged by SDS-PAGE (Supplementary Figure S2). AtPCOs co-purify with substoichiometric levels of Fe (~0.3 Fe atoms/molecule) [7] and inductively coupled plasma mass spectrometry (ICP-MS) analysis of MpPCO and KnPCO samples revealed that these enzymes also bind Fe to substoichiometric levels, at 0.16 (± 0.006) and 0.27 (± 0.013) Fe atoms/molecule, respectively (Supplementary Table S1). These values were used to determine the proportion of active enzyme for subsequent assays. Similar to AtPCO4 [7], both MpPCO and KnPCO also bound Ni (a contaminant of Ni-affinity chromatography) and a low proportion of Zn (Supplementary Table S1).

MpPCO and KnPCO are cysteinyl dioxygenases

To determine whether MpPCO and KnPCO have equivalent functionality to the AtPCOs, both enzymes were incubated with a known AtPCO substrate, a 14-mer peptide representing the N-terminus of the *A. thaliana* ERF-VIIs RAP2.2 and RAP2.12 (herein referred to as AtRAP2_{2-15}). Following 1 hour incubation under atmospheric conditions at 25 °C and subsequent analysis of the mass of the AtRAP2_{2-15} substrate by UPLC-MS, a +32 Da shift was observed in the presence of both MpPCO and KnPCO (Figure 1). This was also dependent on the presence of O_2 as modification did not take place in the presence of 100% N_2 under otherwise equivalent conditions. Tandem MS/MS verified that the modification observed in the presence of O_2 was localised to the N-terminal Cys residue (Supplementary Figure S3). These data are consistent with MpPCO- and KnPCO-catalysed oxidation of AtRAP2_{2-15} Nt-Cys to Cys-sulfinic acid, as observed for all of the the AtPCOs [7]. This demonstrates that both MpPCO and KnPCO are cysteinyl dioxygenases, verifying that, at least *in vitro*, functional PCO enzymes are conserved in early land plants and algae.

MpPCO and KnPCO catalyse oxidation of known AtPCO substrates from angiosperms

The AtPCOs are known to regulate the stability of two other Nt-Cys initiating substrates, AtZPR2 and AtVRN2 [13,14]. Although, like the ERF-VIIs, these substrates are restricted to flowering plants, we nevertheless sought to determine whether peptides representing the N-termini of these substrates could act as substrates for MpPCO and KnPCO. Peptides representing the Cys-initiating N-termini of each of these substrates (herein referred to as AtVRN2_{2-15} and AtZPR2_{2-15}) were incubated for 1 hour in the presence of MpPCO, KnPCO and AtPCO4. For each enzyme, oxidation of all 3 substrates was observed (Figure 2), albeit to differing degrees. AtPCO4 showed considerably greater activity towards AtRAP2_{2-15} (82.6% oxidation) than to AtVRN2_{2-15} (22.6% oxidation) or AtZPR2_{2-15} (11.1% oxidation). MpPCO was most active towards all substrates, showing 86.2% oxidation towards AtRAP2_{2-15}, 89.1% oxidation towards AtVRN2_{2-15} and 74.2% oxidation towards AtZPR2_{2-15}. KnPCO showed a similar substrate selectivity profile to AtPCO4, with greater activity towards AtRAP2_{2-15} (62.8% oxidation) than to AtVRN2_{2-15} (31.9% oxidation) or AtZPR2_{2-15} (7.3% oxidation).

These data indicate that PCO enzymes from different organisms have different substrate selectivity profiles under the conditions tested, with MpPCO showing a particularly robust activity profile towards each substrate. It is important to consider that these are prolonged assays, the results of which may simply reflect the ability of each enzyme to sustain catalytic activity towards each substrate; notably these assays were not supplemented with additional Fe(II) or ascorbate (see below). Furthermore, the proteins represented by the RAP2, ZPR2 and VRN2 peptides are only found within the flowering plants [15], so cannot represent endogenous substrates for MpPCO or KnPCO.

Nevertheless, these results do suggest that PCO enzymes from different organisms could demonstrate divergent substrate selectivity.

MpPCO and KnPCO catalyse oxidation of a peptide representing an Nt-Cys initiating protein from M.polymorpha, 'MpERF-like'.

Given that the substrates tested so far are not physiologically relevant in *M.polymorpha* or *K.nitens*, we next used the online tool Phytozome [21] to probe proteomic data from these organisms to ascertain whether there are any Nt-Cys-initiating sequences with potential homology to known AtPCO substrates. One Met-Cys initiating protein similar to the AtERF-VII substrates was identified in the *M. polymorpha* proteome (transcript ID: Mapoly0293s0001). The protein is a putative AP2/ERF-like transcription factor and, when compared with the AtERF-VII substrates, shares the highest percentage identity with the AtERF-VII Hypoxia Response Element 2 (AtHRE2) at 32.8%. We refer to this protein as 'MpERF-like' to reflect this homology.

A 14-mer peptide representing the Cys-initiating N-terminus of this protein was synthesised (CRMNKRLGKGETGL, hereafter termed MpERF-like$_{2\text{-}15}$) and incubated with MpPCO to determine whether it is a substrate for cysteinyl dioxygenation. Following incubation with MpPCO for 1 hour under atmospheric conditions at 25°C, UPLC-MS analysis revealed a +32 Da shift in the peptide mass, consistent with Nt-Cys oxidation to Cys-sulfinic acid (Figure 3A). Under these conditions, MpPCO-catalysed MpERF-like$_{2\text{-}15}$ oxidation reached 89.3 % (Figure 3B), demonstrating a similar ability to oxidise a potentially endogenous substrate as for substrates from Arabidopsis (though, as discussed above, this may just represent an ability of MpPCO to sustain activity over a prolonged incubation period). The presence of arginyl-tRNA transferase (ATE) and E3 N-recognin, PROTEOLYSIS (PRT) 6 homologs in the *M. polymorpha* proteome supports the potential for an O_2 dependent pathway via the Cys/Arg branch of the N-degron pathway. Our data suggest MpERF-like has the biochemical potential to be regulated via this pathway; *in vivo* studies will be required to confirm whether it is a physiological N-degron pathway target.

Notably, no putative ERF homologues were identified in the *K.nitens* genome, but Blastp searches of the *K. nitens* genome returned ATE and PRT6 homologs, suggesting the potential existence of a functional N-degron pathway. This is consistent with the evolutionary conservation of elements of this pathway, including in most green algae [15]. Both recombinant AtPCO4 and KnPCO were also able to catalyse oxidation of MpERF-like$_{2\text{-}15}$ to 11.6 and 51.4 %, respectively (Figure 3B). Interestingly, KnPCO and AtPCO4 show similar levels of activity towards the peptide substrates originating from Arabidopsis, but KnPCO shows a higher level of activity than AtPCO4 towards MpHRE-like$_{2\text{-}15}$. Physiologically relevant endogenous substrates of KnPCO remain to be identified.

MpPCO and KnPCO have the potential to act as O_2-sensing enzymes

Having demonstrated O_2-dependence of KnPCO and MpPCO activity, we sought to determine whether their rate of activity was dependent on the availability of O_2, and therefore whether they have the potential to act as O_2-sensing enzymes in their respective organisms. For this purpose, kinetic studies of their activity were undertaken with both AtRAP2.12$_{2\text{-}15}$ and MpERF-like$_{2\text{-}15}$ substrates.

Prior to kinetic analysis, assays were conducted to establish optimal conditions for MpPCO and KnPCO activity. Oxidation of both AtRAP2$_{2\text{-}15}$ and MpERF-like$_{2\text{-}15}$ peptides was optimal in the presence of 1 mM tris(2-carboxyethyl)phosphine (TCEP) for both enzymes and optimal buffer pH was found to be pH 8 (Supplementary Figure S4), similar to the AtPCOs [8]. According to the ICP-MS results, neither MpPCO nor KnPCO are fully saturated with a 1:1 ratio of Fe:protein, therefore we investigated whether supplementation with additional Fe and ascorbate would increase the rate of enzymatic

activity, as seen for 2 of the AtPCOs [8]. Fe and ascorbate addition in fact reduced the rate of activity (Supplementary Figure S5), therefore these components were excluded from kinetic assays. Initial rates of PCO activity are therefore calculated per mg of total active enzyme present, with the proportion of active enzyme inferred from the fraction of Fe-occupied enzyme.

We next sought to determine the K_M of each enzyme for both AtRAP2$_{2-15}$ and MpERF-like$_{2-15}$ substrates in order to ascertain conditions for K_M (O_2) assays where peptide substrate concentration was not limiting. In so doing, we noticed that our kinetic data for the reaction of MpPCO with MpERF-like$_{2-15}$ peptide were highly variable in quality when using the high concentrations of peptide necessary for K_M determination (>1 mM). Light scattering experiments identified that the MpPCO enzyme was more prone to aggregation than a form of the enzyme where the N-terminal His$_6$-tag was removed (hereafter MpPCO$_c$, Supplementary Figure S6); MpPCO$_c$ did not show variability at high concentrations of MpERF-like$_{2-15}$, therefore subsequent kinetic analysis for this reaction used MpPCO$_c$. Initial rates of enzyme activity towards both AtRAP2$_{2-15}$ and MpERF-like$_{2-15}$ substrates were determined (Supplementary Figure S7) and used to generate Michaelis–Menten plots (Figure 5) and derive kinetic constants (Table 1).

KnPCO demonstrated a high rate of activity towards MpERF-like$_{2-15}$, with a turnover (k_{cat}) of 43.4 s^{-1}, compared to 18.0 s^{-1} with AtRAP2$_{2-15}$, which appeared to be linked to greater catalytic efficiency with MpERF-like$_{2-15}$ as KnPCO K_M values for AtRAP2$_{2-15}$ and MpERF$_{2-15}$ peptides were 914 and 930 µM, respectively. MpPCO was less active than KnPCO in the presence of both substrates, with turnover numbers of 8.2 s^{-1} and 7.9 s^{-1} with AtRAP2$_{2-15}$ and MpERF-like$_{2-15}$, respectively. MpPCO exhibited substrate inhibition in the presence of >50 µM AtRAP2$_{2-15}$; data fitting to a substrate inhibition model indicated an inhibition constant of 0.28 ± 0.06 mM. The K_M values for MpPCO with the AtRAP2$_{2-15}$ and MpERF-like$_{2-15}$ peptides were 11 and 509 µM respectively; given similar k_{cat} values for these two substrates this suggests a significantly greater binding affinity of this enzyme for AtRAP2$_{2-15}$ over the (potentially) endogenous MpERF$_{2-15}$.

Having identified the optimal concentrations of MpPCO and KnPCO substrate for maximal activity, we next determined their K_M (O_2) values to ascertain whether they have the biochemical potential to act as O_2 sensors. This was done using a method previously described [22]; briefly, reactions were conducted in sealed vials in which solutions had been saturated with gases at different ratios of O_2 and N_2. Reactions were quenched at single time points within the linear rate range (45 – 60 s, Supplementary Figure S7). Peptide oxidation was quantified by LC-MS analysis and the data used to generate Michaelis–Menten kinetic plots from which K_M (O_2) values were derived (Figure 5, Table 1). AtPCOs have previously been reported to have K_M (O_2) values for AtRAP2$_{2-15}$ ranging from 5.45 – 17.3 % O_2 [8]. Interestingly, MpPCO was found to have a lower K_M (O_2) value for this substrate at 3.5% O_2 and a K_M (O_2) value of 8.7 % O_2 for the MpERF-like$_{2-15}$ substrate. The sensitivity of this enzyme to O_2 availability was therefore rather low compared to the Arabidopsis enzymes, suggesting that MpPCO is responsive to changes in O_2 availability when O_2 is already below normoxic levels. In contrast, KnPCO had high K_M (O_2) values towards both substrates: 28.9 and 26.3 % O_2 with AtRAP2$_{2-15}$ and MpERF-like$_{2-15}$, respectively. These K_M (O_2) values are greater than those of any PCO measured to date, suggesting the potential for KnPCO to be highly sensitive to changes in O_2 availability across a wide range of concentrations.

Discussion

In flowering plants, the PCOs have been shown to regulate the genetic response to chronic hypoxia such as those observed during developmental processes [13,14], and acute hypoxia incurred as a result of submergence [6]. PCO-like sequences are ubiquitous throughout the plant kingdom, however the ERF-VII and other known MC-initiating PCO substrates are confined to the flowering plants, with no homologous ERF sequences found in algae. Nevertheless, we and others [15] have identified putative components of the N-degron pathway, PCO, PRT6 and ATE1 homologs, in the *M. polymorpha* and *K. nitens* proteomes and genomes, respectively. This suggests that early land plants and algae also have the potential to regulate Nt-Cys initiating protein stability in an O_2-dependent manner. We have investigated the function of putative PCO enzymes from these organisms. We found that they do indeed act as Nt-Cys dioxygenases and that their activity is sensitive to O_2 availability, particularly KnPCO. This means they have the biochemical potential to act as O_2-sensors. This is the first report of functional PCO enzymes from algae and these findings support an evolutionarily important role for these enzymes [17].

MpPCO and KnPCO have been characterised with respect to their activity towards a peptide representing the N-terminus of a known PCO target from Arabidopsis, the ERF-VII transcription factor RAP2.12 (AtRAP2$_{2\text{-}15}$). We also investigated the activity of both enzymes towards two other PCO substrates which have been identified in Arabidopsis, ZPR2 and VRN2, and compared their activity to that of AtPCO4. Interestingly, over the course of 1 hour of incubation, all 3 PCO enzymes showed relatively high levels of activity towards AtRAP2$_{2\text{-}15}$. However, AtPCO4 and KnPCO showed much lower levels of activity towards AtZPR2$_{2\text{-}15}$ and AtVRN2$_{2\text{-}15}$. This indicates that, under the conditions used, either oxidation of these substrates by AtPCO4 and KnPCO is much slower than oxidation of RAP2$_{2\text{-}15}$, or that AtPCO4 and KnPCO are inactivated during the course of this reaction, possibly by substrate or product inhibition. In contrast, oxidation of AtZPR2$_{2\text{-}15}$ and AtVRN2$_{2\text{-}15}$ was high in the presence of MpPCO. None of these substrates is endogenously present in either *M.polymorpha* or *K.nitens*, meaning these results are not physiologically relevant. However, they do indicate that MpPCO possesses structural features which engender different catalytic and/or substrate binding properties to those of KnPCO and AtPCO4. In a physiological context, these are likely to be important for the endogenous function of MpPCO and could indicate that despite a low K_M O_2, sustained (albeit slow) activity of this enzyme could nevertheless result in significant levels of substrate oxidation.

As well as demonstrating MpPCO and KnPCO function towards a substrate from Arabidopsis, we have identified a putative transcription factor from the *M.polymorpha* proteome which we termed MpERF-like. MpERF-like has an N-terminal Cys residue, but does not have the conserved (M)CGGAI motif synonymous with ERF-VIIs in flowering plants [4]. Nevertheless, we found that MpPCO, KnPCO and also AtPCO4 could all catalyse oxidation of MpERF-like$_{2\text{-}15}$. As observed for the Arabidopsis-derived substrates, MpPCO sustained activity towards this peptide for 1 hour while AtPCO4 and, to a lesser extent KnPCO, showed reduced activity. In steady state kinetic assays, measured under initial rate conditions, both KnPCO and MpPCO demonstrated a higher k_{cat} value for MpERF-like$_{2\text{-}15}$ than they did for AtRAP2$_{2\text{-}15}$ and their activity appeared to be O_2-sensitive, indicating the potential for the corresponding protein to be hypoxically regulated.

While both KnPCO and MpPCO have the biochemical capacity to act as O_2 sensors, both the MpPCO/AtRAP2$_{2\text{-}15}$ and MpPCO/MpERF-like$_{2\text{-}15}$ reactions are sensitive at lower O_2 concentrations, and across a narrower range, than the equivalent KnPCO-catalysed reactions. The low O_2-sensitivity of MpPCO may be physiologically relevant, and it is tempting to speculate that this is related to its poorly oxygenated ecological niche. However, it is possible that PCO O_2-sensitivity is substrate dependent and oxidation of validated endogenous substrates in *M.polymorpha* may prove to have higher K_M (O_2)

values. Furthermore, MpPCO activity towards 14-mer peptides may not be representative of endogenous activity towards full length proteins. It will be interesting to see which proteins are genuinely regulated by the N-degron pathway in *M.polymorpha* and confirm the O_2-sensitivity of this process. Conversely, the activity of KnPCO towards both AtRAP2$_{2\text{-}15}$ and AtERF-like$_{2\text{-}15}$ showed O_2-sensitivity (as determined by K_M (O_2) values) greater than those reported for the AtPCOs [8]. This intriguing result suggests that, if functional at an endogenous level, the N-degron pathway in *K.nitens* could be highly regulated by O_2 availability. It also raises the possibility that structural differences between two enzymes, KnPCO and MpPCO, lead to significant differences in O_2-sensing capability.

Overall this work confirms that *K.nitens* and *M.polymorpha* have the potential for functional, O_2-sensing enzymes which may regulate protein stability in an O_2-dependent manner. While the work is conducted at the biochemical level, and thus does not provide direct evidence for endogenous PCO function in these organisms, we nevertheless demonstrate that such function is a possibility. Our results suggest that further investigation into the role of PCO function in early land plants and algae may reveal novel regulatory features and potentially uncover pathways with differing sensitivity to O_2. Exploring the adaptation and potential levels of O_2 triggers of stress responses in these simple photosynthetic organisms could reveal how different O_2 tolerances emerge depending on ecology and/or complexity and could unveil some of the first steps to the evolution of O_2-sensing function in higher plants.

Materials and Methods

Expression and Purification of MpPCO and KnPCO

The gene encoding MpPCO was amplified from initial constructs donated by Professor Francesco Licausi and cloned into pET28a (Novagen). The gene encoding KnPCO was synthesised and inserted into pET28a (Genscript). Recombinant proteins were expressed and purified as described previously [8]. Briefly, enzymes were expressed in *E. coli* BL21 (DE3) competent cells induced with 0.5 mM isopropyl 1-thio-β-D-galactopyranoside for 16 hours 18 °C. Soluble protein was purified via Ni-affinity chromatography and size exclusion chromatography. Protein purity was assessed by SDS-PAGE.

Peptide Synthesis and Purification

Peptides were either purchased from GL Biochem (China) (AtRAP2$_{2\text{-}15}$ CGGAIISDFIPPPR, AtZPR2$_{2\text{-}15}$ CLTTSEPPFPDTDT, AtVRN2$_{2\text{-}15}$ CRQNCRAKSSPEEV) or synthesised (MpHRE-like$_{2\text{-}15}$, CRMNKRLGKGETGL) using a Liberty Blue™ Microwave Peptide Synthesiser (CEM Corporation), via fluorenylmethyloxycarbonyl (Fmoc) solid phase peptide synthesis using a NovaPEG rink amide resin (Merck). The 14-mer peptides were prepared as C-terminal amides and cleaved from the resin using trifluoracetic acid/water/triisopropylsilane/dimethoxy benzene mix. Peptides were purified using high-performance liquid chromatography and a C18 column.

MpPCO/KnPCO metal content determination

Trace element analyses of metal content in enzyme samples were conducted using inductively coupled plasma mass-spectrometry (ICP-MS) on a NexION 350D ICP-MS (PerkinElmer) coupled with a prepFAST Flow Injection Automation System autosampler (Elemental Scientific). The instrument was calibrated from a series of several standards, which were robotically prepared by the autosampler. Each solution was injected into the instrument nine times at 100ms intervals, and the concentration calculated from the average peak height of the nine injections by comparison to the calibration response curve. Rhodium, indium iridium and rhenium were also added into each measured solution

as internal standards, to correct for any instrumental drift that may be caused by matrix suppression. Ratios of Fe per protein molecule were calculated.

KnPCO/MpPCO activity assays

Unless indicated otherwise, the activities of KnPCO and MpPCO were examined by incubating synthesized peptide with 0.1 µM enzyme at 25 °C under aerobic conditions in the presence of 1 mM TCEP, 50 mM Bis tris propane and 50 mM NaCl at pH as specified in the text. Reactions were quenched by the addition of 1% formic acid. For qualitative analysis, oxidation was monitored by ultrahigh-performance LC (UPLC)-MS using an Acquity UPLC system coupled to a Xevo G2-S Q-ToF mass spectrometer (Waters) operated in positive electrospray mode. Instrument parameters, data acquisition and data processing were controlled by Masslynx 4.1 with source conditions adjusted to maximise sensitivity and minimise fragmentation. Samples were injected on to a Chromolith Performance RP-18e 100^{-2} mm column (Merck) heated to 40 ^{o}C and eluted at 0.3 mL/min using a gradient of 95 % deionized water supplement with 0.1 % (v/v) formic acid to 95 % acetonitrile.

High-throughput steady-state kinetic assays were conducted as described above but were analysed using a RapidFire RF 365 high-throughput sampling robot (Agilent) attached to an iFunnel Agilent 6550 accurate mass quadrupole time-of-flight (Q-TOF) mass spectrometer operating in the positive ionization mode with the parameters: capillary voltage (4000 V), nozzle voltage (1000 V), fragmentor voltage (365 V), gas temperature (225 °C), gas flow (13 L/min), sheath gas temperature (350 °C), sheath gas flow (12 L/min). Samples were aspirated under vacuum for 0.4 s and loaded onto a C4 solid phase extraction (SPE) cartridge at a flow rate of 1.25 mL/min. The C4 SPE was then washed with aqueous 0.1% (v/v) formic acid in LCMS grade water for 5.5 s at a flow rate of 1.25 mL/min followed by elution from the C4 SPE with 85% (v/v) acetonitrile, 15% (v/v) LCMS water containing 0.1% (v/v) formic acid at a flow rate of 1.5 mL/min for 5.5 s. Peptide oxidation was quantified using RapidFire Integrator software (Agilent), where the charged ion with the highest intensity was chosen for deconvolution and peptide quantification. Turnover was quantified by comparing the areas underneath the product and substrate ions. All spectra were assessed manually in Masshunter Qualitative Analysis B.07.00 (Agilent) to ensure the correct ion was chosen for quantification. All figures and kinetic parameters were generated using Prism (GraphPad).

Determining the O_2 Dependence of KnPCO and MpPCO

The activities of KnPCO and MpPCO were examined at different O_2 concentrations using a previously described method [22]. Briefly, silicone-sealed vials containing the desired concentration of peptide and TCEP were equilibrated with different ratios of N_2 and O_2 gas (to give final defined % O_2 concentrations) for 10 min using a mass flow controller (Brooks Instruments). Reactions were initiated by injecting 1.5 µL of enzyme using a gas-tight syringe (Hamilton), incubated at 25 °C for 1 minute and quenched with 80 µL of 1% (v/v) formic acid. Peptide oxidation was analysed by RapidFire Q-TOF MS as described above.

Accession Numbers

MpPCO: PTQ35571; KnPCO: GAQ79467; AtPCO4: Q9SJI9; MpERF-like: A0A2R6VZ45

Acknowledgements

The authors gratefully acknowledge funding from the European Research Council (ERC) under the European Union's Horizon 2020 research and innovation program (PCOMOD project, grant agreement 864888 (EF) and APPELS project, grant agreement no. 681746 (RR)), the U.K. Natural Environmental Research Council (NERC) NE/L002612/1 (LTK) and Wolfson College, Oxford (LTK).

Conflict of interest

The authors declare that they have no conflicts of interest with the contents of this article.

References

[1] D.E. Canfield, R. Raiswell, The evolution of the sulfur cycle, Am. J. Sci. 299 (1999) 697–723. https://doi.org/10.2475/ajs.299.7-9.697.

[2] D.E. Canfield, THE EARLY HISTORY OF ATMOSPHERIC OXYGEN: Homage to Robert M. Garrels, Annu. Rev. Earth Planet. Sci. 33 (2004) 1–36. https://doi.org/10.1146/annurev.earth.33.092203.122711.

[3] D.A. Weits, J.T. van Dongen, F. Licausi, Molecular oxygen as a signaling component in plant development, New Phytol. 229 (2021) 24–35. https://doi.org/10.1111/nph.16424.

[4] J. Bailey-Serres, T. Fukao, D.J. Gibbs, M.J. Holdsworth, S.C. Lee, F. Licausi, P. Perata, L.A.C.J. Voesenek, J.T. van Dongen, Making sense of low oxygen sensing, Trends Plant Sci. 17 (2012) 129–138. https://doi.org/10.1016/j.tplants.2011.12.004.

[5] L.A.C.J. Voesenek, J. Bailey-Serres, Flood adaptive traits and processes: An overview, New Phytol. 206 (2015) 57–73. https://doi.org/10.1111/nph.13209.

[6] D.A. Weits, B. Giuntoli, M. Kosmacz, S. Parlanti, H.-M. Hubberten, H. Riegler, R. Hoefgen, P. Perata, J.T. Van Dongen, F. Licausi, Plant cysteine oxidases control the oxygen-dependent branch of the N-end-rule pathway, Nat. Commun. 5 (2014) 3425. https://doi.org/10.1038/ncomms4425.

[7] M.D. White, M. Klecker, R.J. Hopkinson, D.A. Weits, C. Mueller, C. Naumann, R. O'Neill, J. Wickens, J. Yang, J.C. Brooks-Bartlett, E.F. Garman, T.N. Grossmann, N. Dissmeyer, E. Flashman, Plant cysteine oxidases are dioxygenases that directly enable arginyl transferase-catalysed arginylation of N-end rule targets, Nat. Commun. 8 (2017) 14690. https://doi.org/10.1038/ncomms14690.

[8] M.D. White, J.J.A.G. Kamps, S. East, L.J. Taylor Kearney, E. Flashman, The plant cysteine oxidases from Arabidopsis thaliana are kinetically tailored to act as oxygen sensors, J. Biol. Chem. 293 (2018) 11786–11795. https://doi.org/10.1074/jbc.RA118.003496.

[9] F. Licausi, M. Kosmacz, D.A. Weits, B. Giuntoli, F.M. Giorgi, L.A.C.J. Voesenek, P. Perata, J.T. Van Dongen, Oxygen sensing in plants is mediated by an N-end rule pathway for protein destabilization, Nature. 479 (2011) 419–422. https://doi.org/10.1038/nature10536.

[10] D.J. Gibbs, S.C. Lee, N. Md Isa, S. Gramuglia, T. Fukao, G.W. Bassel, C.S. Correia, F. Corbineau, F.L. Theodoulou, J. Bailey-Serres, M.J. Holdsworth, Homeostatic response to hypoxia is regulated by the N-end rule pathway in plants, Nature. 479 (2011) 415–418. https://doi.org/10.1038/nature10534.

[11] A. Varshavsky, The N-end rule pathway and regulation by proteolysis, Protein Sci. 20 (2011) 1298–1345. https://doi.org/10.1002/pro.666.

[12] M. Garzó, K. Eifler, A. Faust, H. Scheel, K. Hofmann, C. Koncz, A. Yephremov, A. Bachmair, PRT6/At5g02310 encodes an Arabidopsis ubiquitin ligase of the N-end rule pathway with arginine specificity and is not the CER3 locus, FEBS Lett. 581 (2007) 3189–3196. https://doi.org/10.1016/j.febslet.2007.06.005.

[13] D.J. Gibbs, H.M. Tedds, A.-M. Labandera, M. Bailey, M.D. White, S. Hartman, C. Sprigg, S.L. Mogg, R. Osborne, C. Dambire, Oxygen-dependent proteolysis regulates the stability of angiosperm polycomb repressive complex 2 subunit VERNALIZATION 2, Nat. Commun. 9 (2018) 1–11.

[14] D.A. Weits, A.B. Kunkowska, N.C.W. Kamps, K.M.S. Portz, N.K. Packbier, Z. Nemec Venza, C. Gaillochet, J.U. Lohmann, O. Pedersen, J.T. van Dongen, F. Licausi, An apical hypoxic niche sets the pace of shoot meristem activity, Nature. 569 (2019) 714–717. https://doi.org/10.1038/s41586-019-1203-6.

[15] D.A. Weits, L. Zhou, B. Giuntoli, L.D. Carbonare, S. Iacopino, L. Piccinini, V. Shukla, L.T. Bui, G. Novi, J.T. van Dongen, F. Licausi, Acquisition of hypoxia inducibility by oxygen sensing N-terminal cysteine oxidase in spermatophytes, BioRxiv. (2020) 2020.06.24.169417. https://doi.org/10.1101/2020.06.24.169417.

[16] N. Masson, T.P. Keeley, B. Giuntoli, M.D. White, M.L. Puerta, P. Perata, R.J. Hopkinson, E. Flashman, F. Licausi, P.J. Ratcliffe, Conserved N-terminal cysteine dioxygenases transduce responses to hypoxia in animals and plants, Science (80-.). 365 (2019) 65 LP – 69. https://doi.org/10.1126/science.aaw0112.

[17] E.U. Hammarlund, E. Flashman, S. Mohlin, F. Licausi, Oxygen-sensing mechanisms across eukaryotic kingdoms and their roles in complex multicellularity, Science (80-.). 370 (2020) eaba3512. https://doi.org/10.1126/science.aba3512.

[18] R. Ligrone, J.G. Duckett, K.S. Renzaglia, Major transitions in the evolution of early land plants: a bryological perspective, Ann. Bot. 109 (2012) 851–871. https://doi.org/10.1093/aob/mcs017.

[19] K. Hori, F. Maruyama, T. Fujisawa, T. Togashi, N. Yamamoto, M. Seo, S. Sato, T. Yamada, H. Mori, N. Tajima, T. Moriyama, M. Ikeuchi, M. Watanabe, H. Wada, K. Kobayashi, M. Saito, T. Masuda, Y. Sasaki-Sekimoto, K. Mashiguchi, K. Awai, M. Shimojima, S. Masuda, M. Iwai, T. Nobusawa, T. Narise, S. Kondo, H. Saito, R. Sato, M. Murakawa, Y. Ihara, Y. Oshima-Yamada, K. Ohtaka, M. Satoh, K. Sonobe, M. Ishii, R. Ohtani, M. Kanamori-Sato, R. Honoki, D. Miyazaki, H. Mochizuki, J. Umetsu, K. Higashi, D. Shibata, Y. Kamiya, N. Sato, Y. Nakamura, S. Tabata, S. Ida, K. Kurokawa, H. Ohta, Klebsormidium flaccidum genome reveals primary factors for plant terrestrial adaptation, Nat. Commun. 5 (2014) 3978. https://doi.org/10.1038/ncomms4978.

[20] M.D. White, L.D. Carbonare, M.L. Puerta, S. Iacopino, M. Edwards, K. Dunne, E. Pires, C. Levy, M.A. McDonough, F. Licausi, E. Flashman, Structures of Arabidopsis thaliana oxygen-sensing plant cysteine oxidases 4 and 5 enable targeted manipulation of their activity, Proc. Natl. Acad. Sci. U. S. A. 117 (2020) 23140–23147. https://doi.org/10.1073/pnas.2000206117.

[21] D.M. Goodstein, S. Shu, R. Howson, R. Neupane, R.D. Hayes, J. Fazo, T. Mitros, W. Dirks, U. Hellsten, N. Putnam, D.S. Rokhsar, Phytozome: a comparative platform for green plant genomics, Nucleic Acids Res. 40 (2012) D1178–D1186. https://doi.org/10.1093/nar/gkr944.

[22] H. Tarhonskaya, R. Chowdhury, I.K.H. Leung, N.D. Loik, J.S.O. McCullagh, T.D.W. Claridge, C.J. Schofield, E. Flashman, Investigating the contribution of the active site environment to the

slow reaction of hypoxia-inducible factor prolyl hydroxylase domain 2 with oxygen, Biochem. J. 463 (2014) 363–372. https://doi.org/10.1042/BJ20140779.

Tables

Table 1. Steady-state kinetic parameters derived for MpPCO and KnPCO activity towards AtRAP2$_{2-15}$ and MpERF-like$_{2-15}$ Experiments were conducted at atmospheric O_2.

Protein	Substrate	k_{cat}	$K_{M,\ peptide}$	V_{max}
		s^{-1}	μM	$\mu mol\ min^{-1}\ mg^{-1}$
MpPCO	AtRAP2$_{2-15}$	8.2 ± 0.5	11 ± 1.1	17.6 ± 1.1
MpPCO$_c$	MpERF$_{2-15}$	7.9 ± 0.4	509 ± 75	16.96 ± 0.9
KnPCO	AtRAP2$_{2-15}$	18.0 ± 1.2	914 ± 144	36.55 ± 2.4
KnPCO	MpERF$_{2-15}$	43.4 ± 4.3	930 ± 223	87.9 ± 8.7

Table 2. Steady-state kinetic parameters derived for MpPCO and KnPCO activity towards O_2 Experiments were conducted in the presence of non-limiting AtRAP2$_{2-15}$ and MpERF-like$_{2-15}$.

Protein	Substrate	k_{cat}	$K_{M,\ oxygen}$	V_{max}
		s^{-1}	%	$\mu mol\ min^{-1}\ mg^{-1}$
MpPCO	AtRAP2$_{2-15}$	15.5 ± 0.7	3.2 ± 0.6	31.3 ± 1.4
MpPCO$_c$	MpERF$_{2-15}$	18.2 ± 0.9	8.7 ± 1.7	39.1 ± 2.0
KnPCO	AtRAP2$_{2-15}$	59.3 ± 3.7	28.9 ± 4.1	120.2 ± 7.6
KnPCO	MpERF$_{2-15}$	112.2 ± 6.8	26.3 ± 3.8	227.5 ± 13.8

Figures

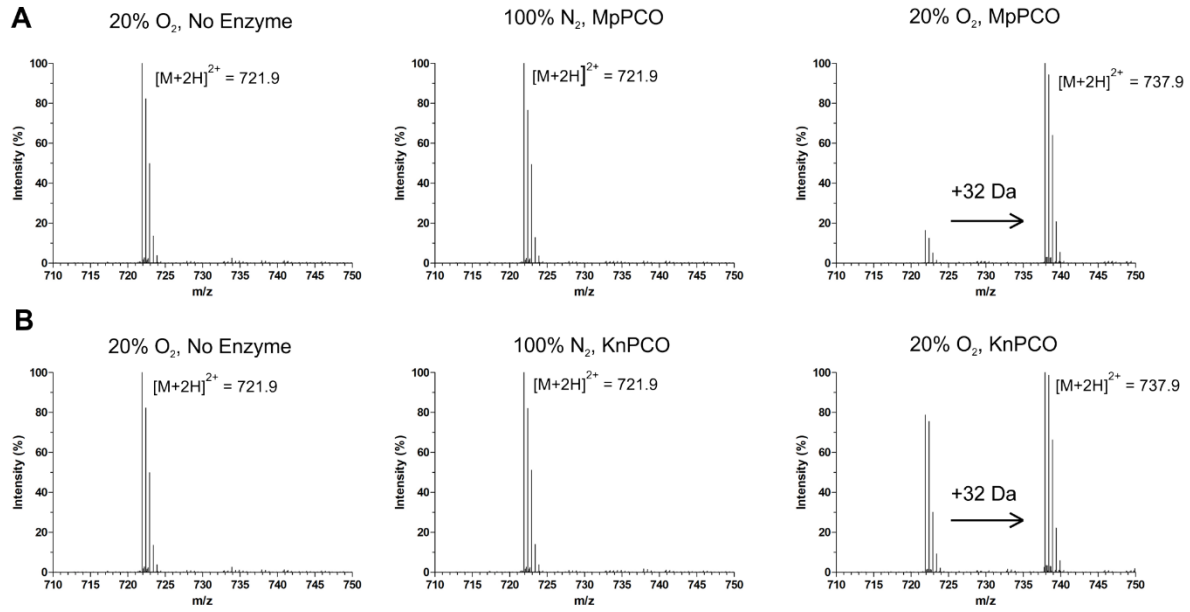

Figure 1. MpPCO and KnPCO catalyse O_2-dependent oxidation of AtRAP2$_{2-15}$ N-terminal Cys. Mass spectra of AtRAP2$_{2-15}$ peptide incubated with and without (**A**) MpPCO or (**B**) KnPCO, under 20% O_2 and under 100% N_2 shows +32 Da increase in the presence of enzyme and O_2, consistent with oxidation. Assays were conducted for 1 hour at 25 °C in the presence of 200 µM AtRAP2$_{2-15}$ using 50 mM Tris/HCl, 0.4 M NaCl, 1 mM TCEP, pH 7.5 as buffer.

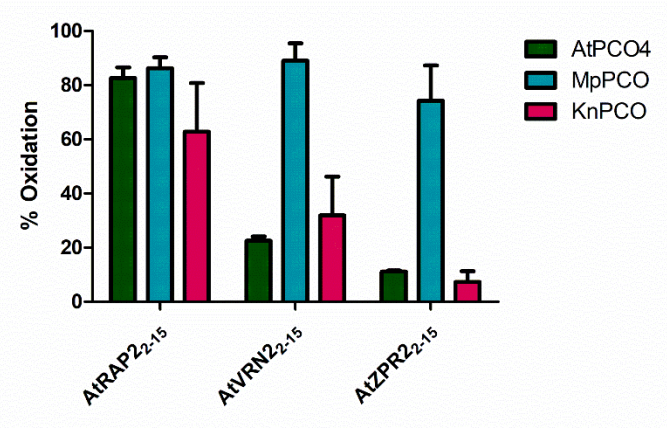

Figure 2. AtPCO4, MpPCO and KnPCO activity with *A. thaliana* PCO substrates: A 1-hour end point assay with peptides representing *A. thaliana* PCO substrates, AtVRN2$_{2\text{-}15}$, AtZPR2$_{2\text{-}15}$ and AtRAP2$_{2\text{-}15}$. Assays were conducted at 25 °C using 50 µM peptide, 50 mM Bis tris propane, 50 mM NaCl, and 1 mM TCEP, pH 8.0, as buffer. Error bars represent S.E. (n = 3).

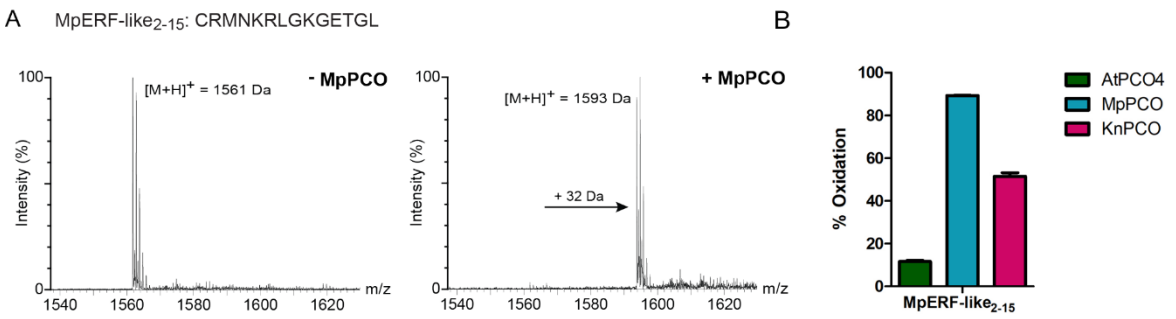

Figure 3. MpPCO and KnPCO catalyse oxidation of MrERF-like$_{2\text{-}15}$. (A) Mass spectra of MpERF-like$_{2\text{-}15}$ peptide (200 µM) incubated with and without MpPCO for 2 minutes at 20% O_2 shows a +32 Da increase in the presence of enzyme, consistent with oxidation. Assays were conducted at 25 °C in the presence of 200 µM AtRAP2$_{2\text{-}15}$ using 50 mM Tris/HCl, 0.4 M NaCl, 1 mM TCEP, pH 7.5 as buffer. **(B)** A 1-hour end point assay comparing activity of AtPCO4, MpPCO and KnPCO towards the MpERF-like$_{2\text{-}15}$ peptide. Assays were conducted at 25 °C using 50 µM peptide, 50 mM Bis tris propane, 50 mM NaCl, and 1 mM TCEP, pH 8.0, as buffer. Error bars represent S.E. (n = 3).

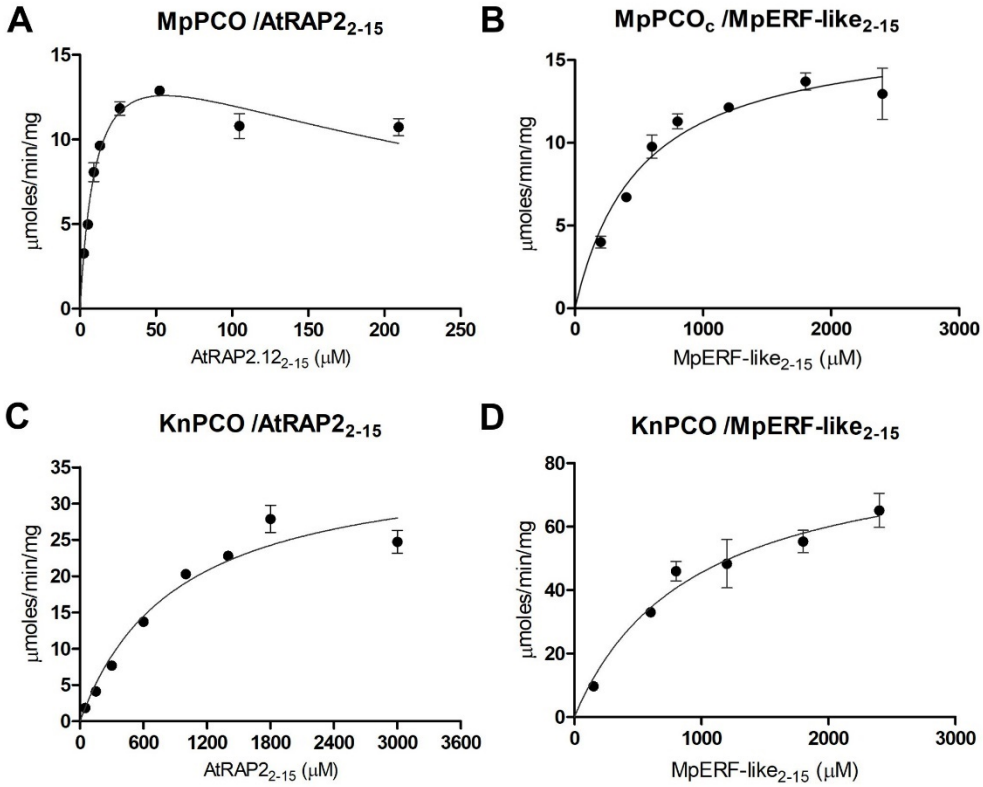

Figure 4. Dependence of MpPCO and KnPCO activity on AtRAP2$_{2-15}$ and MpERF-like$_{2-15}$ availability under atmospheric O_2. Michaelis–Menten kinetic plots for MpPCO and KnPCO activity towards AtRAP2$_{2-15}$ and MpERF-like$_{2-15}$ concentrations are shown. Assays were conducted under aerobic conditions at 25 °C using 50 mM Bis tris propane, 50 mM NaCl, and 1 mM TCEP, pH 8.0, as buffer. Data collected for MpPCO with the AtRAP2$_{2-15}$ and MpERF$_{2-15}$ peptides were fitted to an equation for substrate inhibition to address the decline in rate at higher peptide concentrations. Error bars represent S.E. (n = 3).

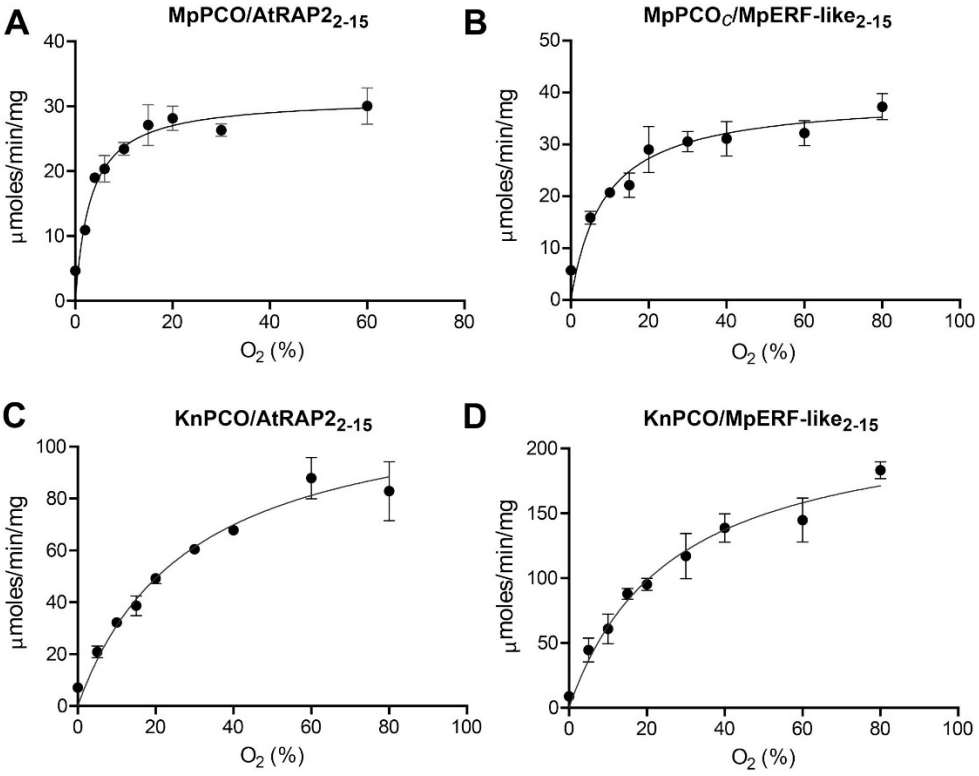

Figure 5. Dependence of MpPCO and KnPCO activity on O_2 availability. Michaelis–Menten kinetic plots for MpPCO and KnPCO with the AtRAP2.12$_{2\text{-}15}$ and MpERF$_{2\text{-}15}$ peptides with respect to varying O_2 availability (solutions saturated with O_2/N_2). Assays were conducted at 25 °C using 50 mM Bis tris propane, 50 mM NaCl, and 1 mM TCEP, pH 8.0, as buffer. Peptide concentrations at the point of maximum activity were chosen to ensure turnover was not limited by peptide availability (Figure 4). Error bars represent S.E. (n = 3).